J. theor. Biol. (2000) **205,** 355–364
doi:10.1006/jtbi.2000.2069, available online at http://www.idealibrary.com on IDEAL®

Insulin Receptor Binding Kinetics: Modeling and Simulation Studies

SUMANAS WANANT AND MICHAEL J. QUON*

Cardiology Branch, National Heart, Lung, and Blood Institute, National Institutes of Health, Bethesda, MD 20892, *U.S.A.*

(*Received on* 22 *November* 1999, *Accepted in revised form on* 31 *March* 2000)

Biological actions of insulin regulate glucose metabolism and other essential physiological functions. Binding of insulin to its cell surface receptor initiates signal transduction pathways that mediate cellular responses. Thus, it is of great interest to understand the mechanisms underlying insulin receptor binding kinetics. Interestingly, negative cooperative interactions are observed at high insulin concentrations while positive cooperativity may be present at low insulin concentrations. Clearly, insulin receptor binding kinetics cannot be simply explained by a classical bimolecular reaction. Mature insulin receptors have a dimeric structure capable of binding two molecules of insulin. The binding affinity of the receptor for the second insulin molecule is significantly lower than for the first bound insulin molecule. In addition, insulin receptor aggregation occurs in response to ligand binding and aggregation may also influence binding kinetics. In this study, we develop a mathematical model for insulin receptor binding kinetics that explicitly represents the divalent nature of the insulin receptor and incorporates receptor aggregation into the kinetic model. Model parameters are based upon published data where available. Computer simulations with our model are capable of reproducing both negative and positive cooperativity at the appropriate insulin concentrations. This model may be a useful tool for helping to understand the mechanisms underlying insulin receptor binding and the coupling of receptor binding to downstream signaling events.

Introduction

The binding of insulin to its cognate cell surface receptor is the initiating step in insulin signaling pathways mediating the promotion of glucose uptake and metabolism (Nystrom & Quon, 1999). Therefore, it is of great interest to understand the mechanisms underlying insulin binding kinetics and their relationship to insulin action. The mature insulin receptor is an integral membrane glycoprotein comprising two extracellular α-subunits and two transmembrane β-subunits linked by disulfide bonds into a heterodimeric structure (Czech, 1985). The α-subunits contain ligand binding regions while the β-subunits contain tyrosine kinase domains that are activated upon ligand binding (for review see Hubbard, 1999; Lee & Pilch, 1994; Zick, 1989). The crystal structure of the tyrosine kinase domain of the insulin receptor has been elucidated (Hubbard, 1997; Hubbard *et al.*, 1994). In addition, the structure of the first three extracellular domains of the related insulin-like growth factor 1 (IGF-1) receptor has been solved (Garrett *et al.*, 1998). This information has recently been used in conjunction with high-resolution imaging by electron cryomicroscopy to generate a three-dimensional quarternary structure for the insulin–insulin receptor complex (Luo *et al.*, 1999).

* Author to whom correspondence should be addressed.
E-mail: quonm@nih.gov

0022–5193/00/150355 + 10 $35.00/0

The kinetics of insulin receptor binding are complex and not well explained by a simple bimolecular reaction such as $H + R \rightleftharpoons HR$ (where H is the free hormone, R is the free receptor, and HR is the hormone–receptor complex) (Gliemann *et al*., 1985; Zick, 1989). Scatchard analyses of equilibrium binding experiments using tracer concentrations of labeled insulin yield curvilinear (upward concave) plots that are typically observed when two classes of binding sites are present (high-affinity low-capacity and low-affinity high capacity) (DeMeyts & Rousseau, 1980; Gliemann *et al*., 1985; Kahn *et al*., 1978b; Pedersen *et al*., 1981). However, because increasing the amount of unlabeled insulin in these binding experiments accelerates the dissociation of labeled insulin, these nonlinear Scatchard plots most likely reflect the presence of negative cooperativity (Christoffersen *et al*., 1994; DeMeyts *et al*., 1976, 1973; DeMeyts & Rousseau, 1980). That is, the affinity of the receptor for insulin decreases as more insulin receptors become occupied. This phenomenon is observed with both purified insulin receptors in a cell-free system as well as with intact cells (Ginsberg *et al*., 1976; Wang *et al*., 1988). Therefore, negative cooperativity is likely to be an intrinsic property of the receptor that is independent of its interactions with other cellular components. Due to its dimeric structure, each insulin receptor molecule is capable of binding to two insulin molecules (Czech, 1985; Pang & Shafer, 1984; Pollet *et al*., 1981, 1982; Yip & Jack, 1992). Interestingly, studies using double-probe labeling techniques suggest that the binding affinity for a second insulin molecule is significantly lower once the first insulin molecule has bound to the receptor (Pang & Shafer, 1983, 1984). This difference between binding affinities for the first and second insulin molecules is one plausible explanation for the negative cooperative binding kinetics of the insulin receptor. An alternative model based upon the ability of insulin to bind and crosslink different surfaces of two α-subunits has also been proposed as a mechanism for negative cooperativity (DeMeyts, 1994; Hammond *et al*., 1997; Schaffer, 1994).

In addition to negative cooperativity, positive cooperativity for insulin receptor binding has been reported at low insulin concentrations (Marsh *et al*., 1984). That is, receptor occupancy seems to enhance binding of insulin to its receptor at low ligand levels. One potential mechanism underlying positive cooperativity is receptor aggregation. Ligand-induced microaggregation or clustering of insulin receptors may be important for insulin internalization and insulin action (Heffetz & Zick, 1986; Hollenberg, 1985; Kahn *et al*., 1978a; Smith *et al*., 1991). Intriguingly, insulin receptor aggregation mediated by anti-receptor antibodies results in enhanced binding of insulin to its receptor in fibroblasts and hepatocytes (Shechter *et al*., 1979). Furthermore, ligands such as epidermal growth factor (EGF) allosterically induce aggregation in their cognate receptors resulting in altered binding affinities (Wofsy *et al*., 1992). Thus, it is conceivable that receptor–receptor interactions may influence receptor–ligand binding kinetics.

In the present study, we develop a mathematical model of insulin receptor binding kinetics that explicitly represents both the divalent nature of insulin receptors and receptor aggregation. With the appropriate parameter choices (based upon published experimental data where available), our model generated computer simulations of both negative and positive cooperativity that mimicked experimental results. Thus, mathematical modeling may be a useful approach for helping to understand the molecular mechanisms underlying the binding of insulin to its receptor.

Model Development

We developed a complex kinetic model for the binding of insulin to its receptor by starting with a simple bimolecular model and incorporating increasing levels of complexity. A system of differential equations was derived for each model that assumed equilibrium states are coupled by first-order rate constants. These model equations were solved simultaneously using a fourth-order Runge–Kutta numerical integration algorithm implemented on a desktop PC (Scraton, 1984). The solutions were considered to be at equilibrium when the absolute values for all derivatives were less than 0.0001. A range of initial ligand concentrations were used to generate computer simulations of equilibrium binding kinetics for each model assuming that the amount of ligand

was in great excess with respect to the receptors. This implies that the concentration of free ligand does not change significantly after equilibrium binding. Cell surface receptor concentration was also assumed to be constant throughout the simulations. That is, receptor trafficking events such as endocytosis, degradation, and recycling were regarded as negligible. This is a reasonable approximation of conditions at 4°C under which most equilibrium binding experiments are performed. For all computer simulations we used a receptor concentration of 1×10^{-10} M and a range of free insulin concentrations from 1×10^{-14} to 1×10^{-6} M. These parameters are consistent with those frequently used in experimental settings (Christoffersen *et al.*, 1994; DeMeyts *et al.*, 1976, 1973; DeMeyts & Rousseau, 1980). We chose to keep the number of receptors constant rather than the number of binding sites because this facilitated comparison of our initial monovalent model with subsequent models that were multivalent. Scatchard analyses of the equilibrium data for each model were plotted (bound/free insulin as a function of bound insulin). When the Scatchard plot is linear, the slope of the line is equal to the negative inverse of the dissociation equilibrium constant while the x-axis intercept is equal to the number of binding sites divided by the dissociation equilibrium constant (Scatchard, 1949).

Bimolecular model—The simplest model for receptor–ligand binding kinetics is represented by the bimolecular reaction

$$\mathrm{H} + \mathrm{R} \underset{k_{-1}}{\overset{k_1}{\rightleftharpoons}} \mathrm{HR},$$

where k_1 is the first-order rate constant for association and k_{-1} is the first order rate constant for dissociation. The equilibrium constant for association is defined as $K_a = k_1/k_{-1}$ and the equilibrium constant for dissociation is defined as $K_d = k_{-1}/k_1$. The differential equations for this model are shown below where $\dot{x} = \mathrm{d}x/\mathrm{d}t$ (derivative of x with respect to time), x_1 is the concentration of free insulin, x_2 the concentration of unbound receptor, and x_3 the concentration of the hormone–receptor complex:

$$\dot{x}_1 = k_{-1}x_3 - k_1 x_1 x_2, \tag{1}$$

$$\dot{x}_2 = k_{-1}x_3 - k_1 x_1 x_2, \tag{2}$$

$$\dot{x}_3 = k_1 x_1 x_2 - k_{-1}x_3. \tag{3}$$

Some investigators have used kinetic experiments to measure k_1 and k_{-1} directly (Corin & Donner, 1982; Pollet *et al.*, 1977), while others have used steady-state experiments to measure K_a or K_d (Gammeltoft & Gliemann, 1973; Hammond *et al.*, 1972; Kahn *et al.*, 1974; Kohanski & Lane, 1983; Pang & Shafer, 1984; Pedersen *et al.*, 1981; Pollet *et al.*, 1981, 1982). There are also investigators who have done both the kinetic and the steady-state experiments on the same preparation in order to validate their results (Gammeltoft *et al.*, 1978; Gliemann *et al.*, 1985; Lipkin *et al.*, 1986a, b). In addition to these labeled-ligand studies, BIAcore surface plasmon resonance has recently been employed to dynamically measure association and dissociation rate constants *in vitro* (Kruse *et al.*, 1997). Reported values for K_a range from $1 \times 10^8\ \mathrm{M}^{-1}$ to $4 \times 10^9\ \mathrm{M}^{-1}$ while values for k_1 range between 3×10^5 and $4 \times 10^6\ \mathrm{M}^{-1}\,\mathrm{s}^{-1}$ and values for k_{-1} range between 1×10^{-4} and $4 \times 10^{-3}\ \mathrm{s}^{-1}$.

Divalent receptor model—To explicitly represent the divalent nature of the insulin receptor we included an additional receptor state where two molecules of insulin are bound to a single receptor (x_4) (Fig. 1). The singly bound and doubly bound insulin receptor states were coupled by first order rate constants for association and dissociation (k_2 and k_{-2}, respectively). The additional equilibrium association constant was defined as $K_2 = k_2/k_{-2}$. The following differential equations describe the divalent receptor model:

$$\dot{x}_1 = k_{-1}x_3 - k_1 x_1 x_2 + k_{-2}x_4 - k_2 x_1 x_3, \tag{4}$$

$$\dot{x}_2 = k_{-1}x_3 - k_1 x_1 x_2, \tag{5}$$

$$\dot{x}_3 = k_1 x_1 x_2 - k_{-1}x_3 + k_{-2}x_4 - k_2 x_1 x_3, \tag{6}$$

$$\dot{x}_4 = k_2 x_1 x_3 - k_{-2}x_4. \tag{7}$$

Receptor aggregation model—To add an additional level of complexity to our model, we next incorporated ligand-induced receptor aggregation (Fig. 2). Several simplifying assumptions

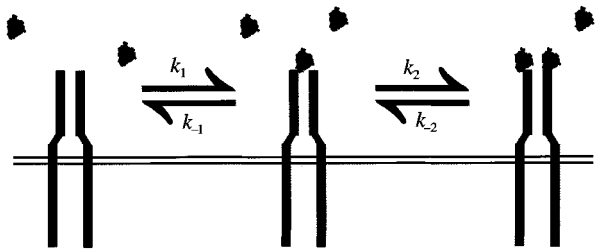

FIG. 1. Schematic diagram of divalent receptor model. k_1 is the association rate constant for insulin and an unbound receptor. k_{-1} is the dissociation rate constant for insulin and a singly bound receptor. k_2 is the association rate constant for insulin and a singly bound receptor. k_{-2} is the dissociation rate constant for insulin and a doubly bound receptor. x_1 = free insulin concentration, x_2 = unbound insulin receptor concentration, x_3 = singly bound receptor concentration, x_4 = doubly bound receptor concentration.

were made to limit the number of receptor states and resulting differential equations. First, receptor aggregation was limited to receptor pair formation. Second, receptors bound to insulin were allowed to aggregate only with unbound receptors (defined by an equilibrium rate constant K_3) (Smith *et al.*, 1991). Third, K_3 was assumed to be the same for receptors with either one or two insulin molecules bound. Fourth, the equilibrium binding constants for receptor aggregates binding additional insulin molecules were assumed to be equivalent for similar states. That is, K_4, the equilibrium binding constant for insulin binding to an unbound half of a receptor aggregate is independent of the number of insulin molecules bound to the other half of the receptor aggregate. Similarly, K_5, the equilibrium binding constant for a second insulin molecule binding to a singly bound half of a receptor aggregate is independent of the number of insulin molecules bound to the other half of the receptor aggregate. Definitions of the various receptor states (x_1–x_9) are given in the legend to Fig. 2. The differential equations governing our receptor aggregation model are shown below:

$$\dot{x}_1 = k_{-1}x_3 - k_1x_1x_2 + k_{-2}x_4 - k_2x_1x_3 + k_{-4}(x_6 + x_7) - k_4x_1(x_5 + x_9) + k_{-5}(x_7 + x_8 + x_9) - k_5x_1 \times (x_5 + x_6 + x_7), \quad (8)$$

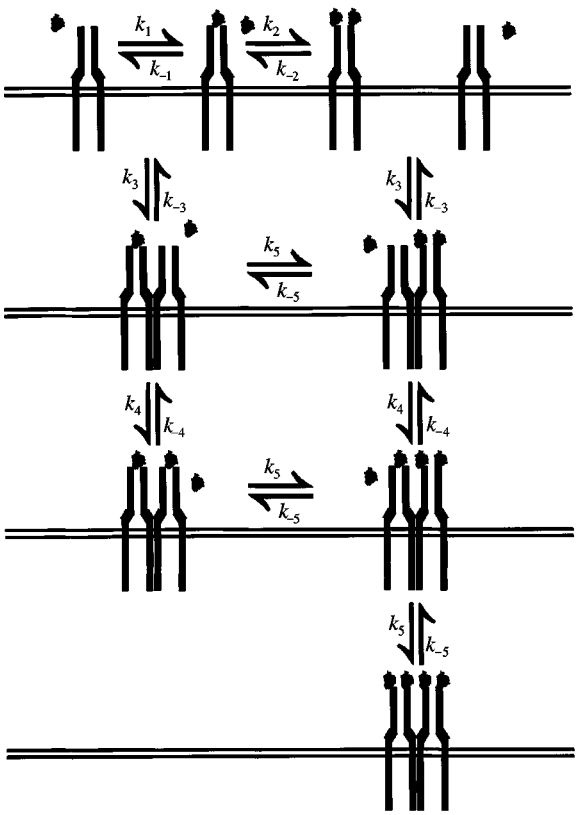

FIG. 2. Schematic diagram of receptor aggregation model. k_1, k_{-1}, k_2, and k_{-2} are defined as in the legend to Fig. 1. k_3 is the aggregation rate constant for a bound receptor aggregating with an unbound receptor. k_{-3} is the dissociation rate constant for receptor aggregates. k_4 is the association rate constant for insulin and an unbound half of a receptor aggregate. k_{-4} is the dissociation rate consant for insulin molecule and a singly bound half of a receptor aggregate. k_5 is the association rate consant for insulin molecule and a singly bound half of a receptor aggregate. k_{-5} is the dissociation rate constant for insulin molecule and a doubly bound half of a receptor aggregate. x_1, x_2, x_3, and x_4 are defined as in the legend to Fig. 1. x_5 is the concentration of unbound–singly bound receptor aggregates. x_6 is the concentration of singly bound–singly bound receptor aggregates. x_7 is the concentration of singly bound–doubly bound receptor aggregates. x_8 is the concentration of doubly bound–doubly bound insulin receptor aggregates. x_9 is concentration of the unbound–doubly bound receptor aggregates.

$$\dot{x}_2 = k_{-1}x_3 - k_1x_1x_2 + k_{-3}(x_5 + x_9) - k_3x_2(x_3 + x_4), \quad (9)$$

$$\dot{x}_3 = k_1x_1x_2 - k_{-1}x_3 + k_{-2}x_4 - k_2x_1x_3 + k_{-3}x_5 - k_3x_2 + x_3, \quad (10)$$

$$\dot{x}_4 = k_2 x_1 x_3 - k_{-2} x_4 + k_{-3} x_9 - k_3 x_2 x_4, \quad (11)$$

$$\dot{x}_5 = k_3 x_2 x_3 - k_{-3} x_5 + k_{-4} x_6 - k_4 x_1 x_5 + k_{-5} x_9 - k_5 x_1 x_5, \quad (12)$$

$$\dot{x}_6 = k_4 x_1 x_5 - k_{-4} x_6 + k_{-5} x_7 - k_5 x_1 x_6, \quad (13)$$

$$\dot{x}_7 = k_4 x_1 x_9 - k_{-4} x_7 + k_{-5}(x_8 - x_7) + k_5 x_1 (x_6 - x_7), \quad (14)$$

$$\dot{x}_8 = k_5 x_1 x_7 - k_{-5} x_8, \quad (15)$$

$$\dot{x}_9 = k_3 x_2 x_4 - k_{-3} x_9 + k_{-4} x_7 - k_4 x_1 x_9 + k_5 x_1 x_5 - k_{-5} x_9. \quad (16)$$

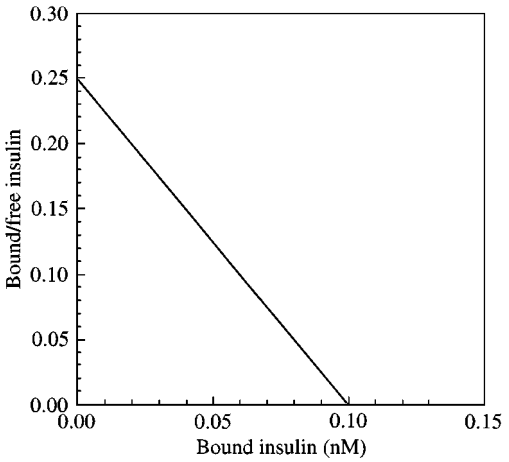

FIG. 3. Scatchard analysis of computer simulation results using the bimolecular model. A receptor concentration of 1×10^{-10} M and a range of free insulin concentrations from 1×10^{-14} to 1×10^{-6} M were used to generate simulation results. $k_1 = 1 \times 10^6\ \mathrm{M^{-1}\,s^{-1}}$; $k_{-1} = 4 \times 10^{-4}\ \mathrm{s^{-1}}$; $K_1 = k_1/k_{-1}$.

Results

The binding of insulin to its receptor has been measured under various conditions in many cell types (including adipocytes, lymphocytes, hepatocytes, and myocytes) as well as in cell-free preparations. The exact values for the kinetic and equilibrium rate constants are dependent upon factors such as cell type, temperature, pH, and ionic composition of the culture media (Gliemann *et al.*, 1985; Kahn, 1976). For our computer simulations we chose representative rate constants that were consistent with the published literature, a receptor concentration of 1×10^{-10} M, and a range of free insulin concentrations from 1×10^{-14} to 1×10^{-6} M.

Bimolecular model—We chose kinetic rate constants of $k_1 = 1 \times 10^6\ \mathrm{M^{-1}\,s^{-1}}$ and $k_{-1} = 4 \times 10^{-4}\ \mathrm{s^{-1}}$ corresponding to an equilibrium assocation constant of $K_1 = 2.5 \times 10^8\ \mathrm{M^{-1}}$ for the bimolecular model. As expected, this classical model generated a linear Scatchard plot that did not conform to the curvilinear Scatchard plots usually associated with insulin binding experiments (Fig. 3). Thus, this simple model is unable to explain the complex binding kinetics of insulin with its receptor.

Divalent model—Based upon double-probe labeling experiments, the equilibrium constant for binding of a second insulin molecule to a receptor with one insulin molecule already bound (K_2) is $\sim$100-fold less than the equilibrium constant for binding the initial insulin molecule (K_1) (Pang & Shafer, 1984). Since accelerated dissociation of labeled ligand has been observed in the presence of unlabeled ligand (DeMeyts *et al.*, 1976), we determined this relationship between K_1 and K_2 by defining $k_{-2} = 100k_{-1}$ and $k_2 = k_1$. Thus, $K_2 = 0.01K_1$. The values chosen for k_1 and k_{-1} were the same as those used for the bimolecular model. Under these conditions, the divalent model generates an upward concave Scatchard plot consistent with the presence of negative cooperativity and similar to experimentally derived Scatchard plots (Fig. 4).

Receptor aggregation model—We added another level of complexity to our divalent receptor model by explicitly representing effects of receptor aggregation on binding kinetics. To simplify the number of possible effects of aggregation on binding kinetics, receptor aggregation was represented by a single equilibrium rate constant K_3. Similar to the relationship between K_1 and K_2 in the divalent receptor model, we chose $K_4 = 100K_5$. That is, there is decreased binding affinity of a second molecule of insulin for a receptor in an aggregate that is already occupied by one insulin molecule. Because the equilibrium constants K_3, K_4, and K_5 have not been

experimentally measured, we tested a range of values for these constants and generated representative Scatchard plots (Figs 5 and 6). Since receptor aggregation occurs upon binding of insulin to its receptor (Heffetz & Zick, 1986; Hollenberg, 1985; Kahn *et al.*, 1978a; Smith *et al.*, 1991), we have assumed that K_3 is of the same order of magnitude as K_1. When the effect of receptor aggregation on binding affinity was neutral (i.e. $K_4 = K_1$) or receptor aggregation was neglected (i.e. $K_3 = 0$), the Scatchard plots resembled those derived from the divalent model and exhibited only negative cooperativity. However, when the binding affinity of insulin for its receptor was enhanced after receptor aggregation (i.e. $K_4 > K_1$), downward concavity in the Scatchard plot was observed at small values of bound insulin implying positive cooperative behavior at low insulin concentrations. In our computer simulations, positive cooperativity appears at bound insulin concentrations below ~ 0.02 nM. The downward concave shape of the Scatchard curve is hardly detectable at higher concentrations. Under these conditions, high insulin concentrations were still associated with negative cooperativity. As the aggregation constant K_3 was increased, the positive cooperative effects became more pronounced. Thus, our receptor aggregation model generates both negative and positive cooperative insulin receptor binding behavior at the appropriate insulin concentrations consistent with the published literature.

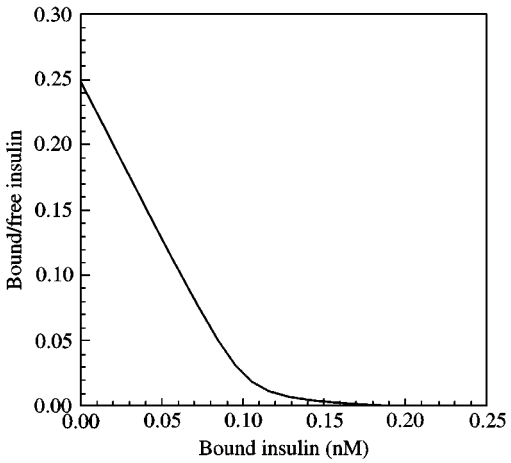

FIG. 4. Scatchard analysis of computer simulation results using divalent receptor model. A receptor concentration of 1×10^{-10} M and a range of free insulin concentrations from 1×10^{-14} to 1×10^{-6} M were used to generate simulation results. $k_1 = 1 \times 10^6\ \mathrm{M^{-1}\,s^{-1}}$; $k_{-1} = 4 \times 10^{-4}\ \mathrm{s^{-1}}$; $K_1 = k_1/k_{-1}$; $k_2 = k_1$; $k_{-2} = 100k_{-1}$; $K_2 = k_2/k_{-2} = 0.01K_1$.

Discussion

The mathematical models of insulin receptor binding kinetics presented here are based upon plausible molecular mechanisms that have been postulated from available experimental data. Our simplest bimolecular model is clearly not sufficient to explain the complex insulin binding kinetics observed experimentally. The structure of our divalent receptor model is based on experiments using a double probe labeling technique to

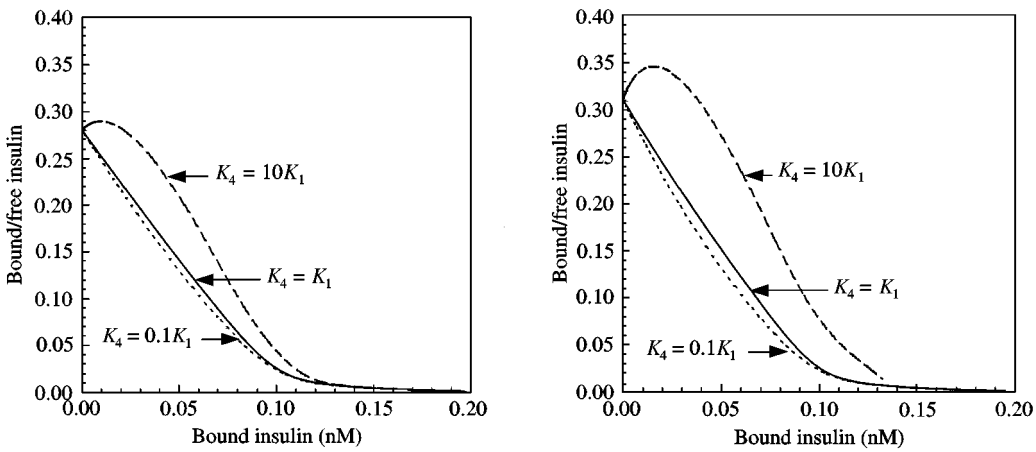

FIG. 5. Scatchard analyses of computer simulation results using receptor aggregation model showing effects of changes in K_4 and K_3. Values for k_1, k_{-1}, k_2, and k_{-2} defined in Fig. 4 were used for all simulations. $K_5 = 0.01K_4$; $K_3 = 0.5\,K_1$ for left panel, $K_3 = K_1$ for right panel.

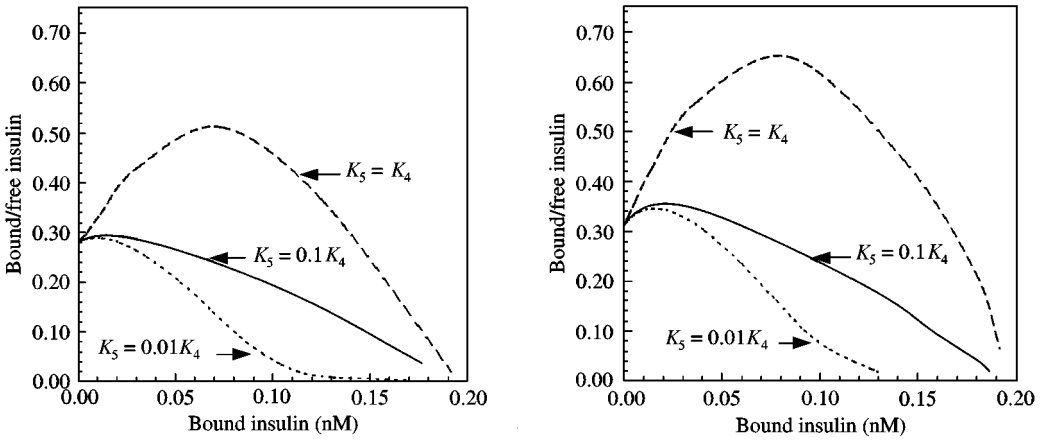

FIG. 6. Additional Scatchard analyses of computer simulation results using receptor aggregation model showing effects of changes in K_5 and K_3. Values for k_1, k_{-1}, k_2, and k_{-2} defined in Fig. 4 were used for all simulations. $K_3 = K_1$; $K_4 = 10K_1$.

show that the binding affinity of a second molecule of insulin to a receptor already bound to one insulin molecule is approximately 100th the affinity of the binding of the first molecule of insulin (Pang & Shafer, 1984). Recent high-resolution imaging of insulin/receptor complexes showing that receptors with two insulin molecules bound are seen much less frequently than receptors bound to a single insulin molecule is also consistent with this model (Luo *et al.*, 1999). Our divalent receptor model is sufficient to explain negative cooperative insulin receptor binding kinetics and generate curvilinear Scatchard plots that are typical of those obtained experimentally.

A number of alternative models proposed by other investigators can also generate upward concave Scatchard plots. For example, a mobile receptor hypothesis proposes that receptor and effector molecules diffuse and interact freely in the plane of the plasma membrane (Jacobs & Cuatrecasas, 1976, 1985). The coordinated interactions of insulin, receptor, and effector molecules can generate curvilinear Scatchard plots and accelerated dissociation curves in the presence of increasing concentrations of unlabeled ligand. However, the fact that purified insulin receptors exhibit negative cooperative binding kinetics independent of the plasma membrane suggests that this behavior is an intrinsic feature of the insulin receptor independent of the plasma membrane (Ginsberg *et al.*, 1976; Wang *et al.*, 1988). DeMeyts and colleagues originally proposed a tetrameric arrangement of insulin receptors similar to that of hemoglobin to explain negative cooperativity in insulin receptor binding kinetics (DeMeyts *et al.*, 1976; Ginsberg *et al.*, 1976). This model is problematic because there is no experimental evidence that insulin receptors interact in groups of four. More recently, models based on the ability of different surfaces of insulin to bind and crosslink distinct regions of the receptor α-subunits have suggested another mechanism for generating negative cooperativity (DeMeyts, 1994; Schaffer, 1994). These models hypothesize two binding surfaces on the insulin molecule that interact with separate binding sites of different affinities (α_1 and α_2) on the two halves of the insulin receptor. Consistent with these models, electron cryomicroscopy studies of a single insulin molecule bound to its receptor demonstrate contact between two different surfaces of insulin and different regions of the two α-subunits contained in each receptor (Luo *et al.*, 1999). While these models can explain the equilibrium binding data, further analysis has shown that the kinetics of accelerated dissociation in the presence of excess unlabeled ligand is not well explained by these models at insulin concentrations in the physiological range (Hammond *et al.*, 1997). In addition, these models are not capable of producing positive cooperative behavior at low insulin concentrations.

To account for their experimental finding of positive cooperativity at low insulin concentrations, Marsh *et al.* proposed that the second

binding site for insulin on each insulin receptor may have enhanced affinity (Marsh *et al*., 1984). The difficulty with this model is that it cannot simultaneously account for both negative and positive cooperativity at the appropriate insulin concentrations. Furthermore, there is no experimental evidence demonstrating enhanced affinity of the second binding site. Our receptor aggregation model takes into account both the divalent nature of insulin receptors and insulin-induced receptor aggregation to produce both negative and positive cooperativity at the appropriate insulin concentrations within a single model. As mentioned in the Introduction, a variety of experimental evidence suggests that receptor aggregation may influence insulin binding kinetics. However, these changes have not been quantified. As expected, when model parameters are chosen to neglect receptor aggregation (i.e. $K_3 = 0$) the binding simulations resemble those of the divalent receptor model. Interestingly, although our modeling of receptor aggregation contains several simplifying assumptions, it is sufficient to generate positive cooperativity at low insulin concentrations consistent with experimental results while preserving the negative cooperative behavior at higher insulin concentrations. The relationship between aggregation and positive cooperativity in this model results from the fact that receptor aggregation (i.e. $K_3 > 0$) gives access to other ligand binding states defined by K_4 and K_5. If receptor aggregates have higher affinity for ligand than unaggregated receptors, positive cooperativity will result from receptor aggregation. This is illustrated in Fig. 5, showing that positive cooperativity is exhibited only when $K_4 > K_1$. It is possible that one might devise a model to explain both positive and negative cooperativity on the basis of receptor aggregation alone (without invoking the divalent nature of the receptor). However, such a model would be extremely implausible because purified receptor preparations that do not undergo receptor aggregation still exhibit negative cooperative binding behavior (Wang *et al*., 1988).

The magnitude of insulin's biological effects is proportional to the number of receptors occupied by insulin. Receptor occupancy is determined by the binding kinetics. However, maximal receptor occupancy is not usually required for maximal biological effect and the number of "spare receptors" present varies depending on the particular action of insulin being studied. Thus, the coupling of receptor occupancy to downstream effects is also an important determinant of insulin action and insulin sensitivity. Insulin resistance (decreased sensitivity or responsiveness to metabolic actions of insulin) may result from a combination of receptor and post-receptor defects and contributes importantly to the pathophysiology of diseases such as obesity and diabetes mellitus (DeFronzo, 1988). In addition to exploring insulin receptor binding kinetics, integrating our receptor aggregation model with other models of insulin receptor and glucose transporter trafficking events (Quon & Campfield, 1991a, b) may give useful insights into the molecular mechanisms underlying insulin action and insulin resistance.

REFERENCES

Christoffersen, C. T., Bornfeldt, K. E., Rotella, C. M., Gonzales, N., Vissing, H., Shymko, R. M., ten Hoeve, J., Groffen, J., Heisterkamp, N. & De Meyts, P. (1994). Negative cooperativity in the insulin-like growth factor-I receptor and a chimeric IGF-I/insulin receptor. *Endocrinology* **135,** 472–475.

Corin, R. E. & Donner, D. B. (1982). Insulin binding to liver plasma membranes from rats rendered diabetic by alloxan. A kinetic demonstration of two classes of binding sites in equilibrium with each other. *Biochem. J*. **202,** 259–262.

Czech, M. P. (1985). The nature and regulation of the insulin receptor: structure and function. *Annu. Rev. Physiol*. **47,** 357–381.

DeFronzo, R. A. (1988). Lilly lecture 1987. The triumvirate: beta-cell, muscle, liver. A collusion responsible for NIDDM. *Diabetes* **37,** 667–687.

DeMeyts, P. (1994). The structural basis of insulin and insulin-like growth factor-I receptor binding and negative co-operativity, and its relevance to mitogenic versus metabolic signalling. *Diabetologia* **37**(Suppl 2), S135–S148.

DeMeyts, P. & Rousseau, G. G. (1980). Receptor concepts. A century of evolution. *Circ. Res*. **46,** I3–I9.

DeMeyts, P., Roth, J., Neville, Jr., D. M., Gavin, J. R. D. & Lesniak, M. A. (1973). Insulin interactions with its receptors: experimental evidence for negative cooperativity. *Biochem. Biophys. Res. Commun*. **55,** 154–161.

DeMeyts, P., Bainco, A. R. & Roth, J. (1976). Site-site interactions among insulin receptors. Characterization of the negative cooperativity. *J. Biol. Chem*. **251,** 1877–1888.

Gammeltoft, S. & Gliemann, J. (1973). Binding and degradation of 125I-labelled insulin by isolated rat fat cells. *Biochim. Biophys. Acta*. **320,** 16–32.

Gammeltoft, S., Kristensen, L. O. & Sestoft, L. (1978). Insulin receptors in isolated rat hepatocytes. Reassessment of binding properties and observations of the inactivation of insulin at 37 degrees C. *J. Biol. Chem*. **253,** 8406–8413.

GARRETT, T. P., MCKERN, N. M., LOU, M., FRENKEL, M. J., BENTLEY, J. D., LOVRECZ, G. O., ELLEMAN, T. C., COSGROVE, L. J. & WARD, C. W. (1998). Crystal structure of the first three domains of the type-1 insulin-like growth factor receptor. *Nature* **394,** 395–399.

GINSBERG, B. H., KAHN, C. R. & ROTH, J. (1976). The insulin receptor of the turkey erythrocyte. Characterization of the membrane-bound receptor. *Biochim. Biophys. Acta.* **443,** 227–242.

GLIEMANN, J., FOLEY, J. E., SONNE, O. & LAURSEN, A. L. (1985). Insulin–receptor interactions. In: *Polypeptide Hormone Receptors* Posner, B. I., (ed.), pp. xviii, 599. New York: Dekker.

HAMMOND, J. M., JARETT, L., MARIZ, I. K. & DAUGHADAY, W. H. (1972). Heterogeneity of insulin receptors on fat cell membranes. *Biochem. Biophys. Res. Commun.* **49,** 1122–1128.

HAMMOND, B. J., TIKERPAE, J. & SMITH, G. D. (1997). An evaluation of the cross-linking model for the interaction of insulin with its receptor. *Am. J. Physiol.* **272,** E1136–E1144.

HEFFETZ, D. & ZICK, Y. (1986). Receptor aggregation is necessary for activation of the soluble insulin receptor kinase. *J. Biol. Chem.* **261,** 889–894.

HOLLENBERG, M. D. (1985). Receptor dynamics and insulin action. In: *Insulin*: *Its Receptor and Diabetes*. Hollenberg, M. D. (ed.), pp. x, 318. New York: M. Dekker.

HUBBARD, S. R. (1997). Crystal structure of the activated insulin receptor tyrosine kinase in complex with peptide substrate and ATP analog. *Embo. J.* **16,** 5572–5581.

HUBBARD, S. R. (1999). Structural analysis of receptor tyrosine kinases. *Prog. Biophys. Mol. Biol.* **71,** 343–358.

HUBBARD, S. R., WEI, L., ELLIS, L. & HENDRICKSON, W. A. (1994). Crystal structure of the tyrosine kinase domain of the human insulin receptor. *Nature* **372,** 746–754.

JACOBS, S. & CUATRECASAS, P. (1976). The mobile receptor hypothesis and "cooperativity" of hormone binding. Application to insulin. *Biochim. Biophys. Acta.* **433,** 482–495.

JACOBS, S. & CUATRECASAS, P. (1985). The mobile receptor hypothesis and polypeptide hormone action. In: *Polypeptide Hormone Receptors*. Posner, B. I., (ed.), pp. xviii, 599. New York: Dekker.

KAHN, C. R. (1976). Membrane receptors for hormones and neurotransmitters. *J. Cell. Biol.* **70,** 261–286.

KAHN, C. R., FREYCHET, P., ROTH, J. & NEVILLE Jr., D. M. (1974). Quantitative aspects of the insulin-receptor interaction in liver plasma membranes. *J. Biol. Chem.* **249,** 2249–2257.

KAHN, C. R., BAIRD, K. L., JARRETT, D. B. & FLIER, J. S. (1978a). Direct demonstration that receptor crosslinking or aggregation is important in insulin action. *Proc. Nat. Acad. Sci. U.S.A.* **75,** 4209–4213.

KAHN, C. R., GOLDFINE, I. D., NEVILLE Jr., D. M. & DE MEYTS, P. (1978b). Alterations in insulin binding induced by changes *in vivo* in the levels of glucocorticoids and growth hormone. *Endocrinology* **103,** 1054–1066.

KOHANSKI, R. A. & LANE, M. D. (1983). Binding of insulin to solubilized insulin receptor from human placenta. Evidence for a single class of noninteracting binding sites. *J. Biol. Chem.* **258,** 7460–7468.

KRUSE, V., JENSEN, I., PERMIN, L. & HEDING, A. (1997). Fate of insulin analogs in intact and nephrectomized rats determined by their receptor binding constants. *Am. J. Physiol.* **272,** E1089–E1098.

LEE, J. & PILCH, P. F. (1994). The insulin receptor: structure, function, and signaling. *Am. J. Physiol.* **266,** C319–C334.

LIPKIN, E. W., TELLER, D. C. & DE HAEN, C. (1986a). Equilibrium binding of insulin to rat white fat cells at 15°C. *J. Biol. Chem.* **261,** 1694–1701.

LIPKIN, E. W., TELLER, D. C. & DE HAEN, C. (1986b). Kinetics of insulin binding to rat white fat cells at 15°C. *J. Biol. Chem.* **261,** 1702–1711.

LUO, R. Z., BENIAC, D. R., FERNANDES, A., YIP, C. C. & OTTENSMEYER, F. P. (1999). Quaternary structure of the insulin–insulin receptor complex. *Science* **285,** 1077–1080.

MARSH, J. W., WESTLEY, J. & STEINER, D. F. (1984). Insulin–receptor interactions. Presence of a positive cooperative effect. *J. Biol. Chem.* **259,** 6641–6649.

NYSTROM, F. H. & QUON, M. J. (1999). Insulin signalling: metabolic pathways and mechanisms for specificity. *Cell. Signal.* **11,** 563–574.

PANG, D. T. & SHAFER, J. A. (1983). Stoichiometry for the binding of insulin to insulin receptors in adipocyte membranes. *J. Biol. Chem.* **258,** 2514–2518.

PANG, D. T. & SHAFER, J. A. (1984). Evidence that insulin receptor from human placenta has a high affinity for only one molecule of insulin. *J. Biol. Chem.* **259,** 8589–8596.

PEDERSEN, O., HJOLLUND, E., BECK-NIELSEN, H., LINDSKOV, H. O., SONNE, O. & GLIEMANN, J. (1981). Insulin receptor binding and receptor-mediated insulin degradation in human adipocytes. *Diabetologia* **20,** 636–641.

POLLET, R. J., STANDAERT, M. L. & HAASE, B. A. (1977). Insulin binding to the human lymphocyte receptor. Evaluation of the negative cooperativity model. *J. Biol. Chem.* **252,** 5828–5834.

POLLET, R. J., HAASE, B. A. & STANDAERT, M. L. (1981). Characterization of detergent-solubilized membrane proteins. Hydrodynamic and sedimentation equilibrium properties of the insulin receptor of the cultured human lymphoblastoid cell. *J. Biol. Chem.* **256,** 12118–12126.

POLLET, R. J., KEMPNER, E. S., STANDAERT, M. L. & HAASE, B. A. (1982). Structure of the insulin receptor of the cultured human lymphoblastoid cell IM-9. Evidence suggesting that two subunits are required for insulin binding. *J. Biol. Chem.* **257,** 894–898.

QUON, M. J. & CAMPFIELD, L. A. (1991a). A mathematical model and computer simulation study of insulin receptor regulation. *J. theor. Biol.* **150,** 59–72.

QUON, M. J. & CAMPFIELD, L. A. (1991b). A mathematical model and computer simulation study of insulin sensitive glucose transporter regulation. *J. theor. Biol.* **150,** 93–107.

SCATCHARD, G. (1949). The attractions of proteins for small molecules and ions. *Ann. NY. Acad. Sci.* **51,** 660–672.

SCHAFFER, L. (1994). A model for insulin binding to the insulin receptor. *Eur. J. Biochem.* **221,** 1127–1132.

SCRATON, R. E. (1984). *Basic Numerical Methods*: *an Introduction to Numerical Mathematics on a Microcomputer*. London; Baltimore, MD, U.S.A.: E. Arnold.

SHECHTER, Y., CHANG, K. J., JACOBS, S. & CUATRECASAS, P. (1979). Modulation of binding and bioactivity of insulin by anti-insulin antibody: relation to possible role of receptor self-aggregation in hormone action. *Proc. Nat. Acad. Sci. U.S.A.* **76,** 2720–2724.

SMITH, R. M., SEELY, B. L., SHAH, N., OLEFSKY, J. M. & JARETT, L. (1991). Tyrosine kinase-defective insulin

receptors undergo insulin-induced microaggregation but do not concentrate in coated pits. *J. Biol. Chem.* **266,** 17522–17530.

WANG, C. C., GOLDFINE, I. D., FUJITA-YAMAGUCHI, Y., GATTNER, H. G., BRANDENBURG, D. & DE MEYTS, P. (1988). Negative and positive site-site interactions, and their modulation by pH, insulin analogs, and monoclonal antibodies, are preserved in the purified insulin receptor. *Proc. Nat. Acad. Sci. U.S.A.* **85,** 8400–8404.

WOFSY, C., GOLDSTEIN, B., LUND, K. & WILEY, H. S. (1992). Implications of epidermal growth factor (EGF) induced egf receptor aggregation. *Biophys. J.* **63,** 98–110.

YIP, C. C. & JACK, E. (1992). Insulin receptors are bivalent as demonstrated by photoaffinity labeling. *J. Biol. Chem.* **267,** 13131–13134.

ZICK, Y. (1989). The insulin receptor: structure and function. *Crit. Rev. Biochem. Mol. Biol.* **24,** 217–269.